Dyes and Pigments 92 (2011) 588–595

Contents lists available at ScienceDirect

Dyes and Pigments

journal homepage: www.elsevier.com/locate/dyepig

High efficient and high color pure blue light emitting materials: New asymmetrically highly twisted host and guest based on anthracene

Il Kang [a], Jang-Yeol Back [c], Ran Kim [b], Yun-Hi Kim [b],*, Soon-Ki Kwon [a],*

[a] School of Materials Science and Engineering & Engineering Research Institute (ERI), Gyeongsang National University, Jinju-660 701, South Korea
[b] Department of Chemistry and Research Institute of Natural Sciences (RINS), Gyeongsang National University, Jinju-660 701, South Korea
[c] EL Materials Development Division Duksan Hi-Metal Co., Bundang 463-420, South Korea

ARTICLE INFO

Article history:
Received 15 March 2011
Received in revised form
6 June 2011
Accepted 7 June 2011
Available online 21 June 2011

Keywords:
Organic light emitting diodes
Asymmetrically highly twisted anthracene derivative
Blue emission
Color purity
High efficiency
Matched host-guest

ABSTRACT

New asymmetrically highly twisted anthracene derivatives serve as a matched host and guest material in high efficiency blue OLEDs. 2-(2-Methylnaphtathalene-1-yl)-9,10-di(naphthalene-2-yl)anthracene and *N*-(4-(10-naphthalene-2-yl)anthracene-9-yl)phenyl-*N*-phenylnaphthalene-2-amine were prepared as host material and as guest material, respectively. Multilayer organic electroluminecent devices constructed using these foregoing twisted anthracene derivatives as the emitting layer gave quantum efficiencies of 5% and exhibited a pure blue emission with CIE chromaticity coordinates $x = 0.15$, $y = 0.14–0.18$.

1. Introduction

Organic light emitting devices (OLEDs) have been attracting considerable attention for potential application in flat-panel displays [1,2]. Efficient blue-light OLEDs are of particular interest, because they are desired for use as blue light sources in full color display applications [3–8]. Significant progress in materials synthesis and device construction has led to the realization of full color as well as white OLEDs with improved efficiencies and lifetimes [9]. Extensive efforts have been made to develop high performance materials with desirable properties, and devices with optimized architectures to develop marketable OLEDs [10]. Fluorophores with attractive emission characteristics such as a good range of colors, and high efficiency are desired as emitters of OLEDs. Furthermore, the realization of a thermally and morphologically stable amorphous film is another important factor that can drastically improve the physical performance of OLEDs [11]. Given this background, the development of high performance blue-emitting materials is a subject of current interest [12–14]. This is especially true for a deep-blue color, which is usually defined as blue electroluminescent emission having Commission Internationale de l'Enclairage (CIE) coordinates (*y*-coordinate value < 0.15) [15]. Guest/host systems have been demonstrated as a approach to achieve high efficiency and color purity, and much work has been undertaken in developing the guest and host materials and their combinations. Generally, a good host material should possess a wide energy gap, good carrier transporting abilities and film forming abilities. The most widely used host materials involve di(styryl)arylene derivatives and anthracene derivatives [16]. The guest materials should possess high luminescent efficiency as well as the ability to accept energy from host materials via the Foster energy transfer and/or direct recombination via charge trapping [17].

Many efficient blue emitting materials for hosts and guests have been designed, such as anthracene [18–25], fluorene [26], di(styryl)arylene [27], tetra(phenyl)pyrene [28] and tetra(phenyl)silyl derivatives [29]. As part of our ongoing efforts to search for robust materials for full color OLED display devices, we recently submitted a highly twisted asymmetric anthracene derivative, 2-(2-methylnaphthalene)-9,10-di(naphthalene-2-yl)anthracene (MNAn), which was an efficient blue color emitter [30].

---

* Corresponding authors. Tel.: +82 55 751 5296.
E-mail addresses: ykim@gnu.ac.kr (Y.-H. Kim), skwon@gnu.ac.kr (S.-K. Kwon).

0143-7208/$ – see front matter © 2011 Elsevier Ltd. All rights reserved.
doi:10.1016/j.dyepig.2011.06.008

In this paper, we studied the highly twisted asymmetric 2-(2-methylnaphthalene-)-9,10-di(naphthalene-2-yl)anthracene as a wide energy gap host for blue OLEDs. Although the 9,10-di(naphthalene-2-yl)lanthracene (ADN) and 2-(2-methylnaphthalene)-9,10-di(naphthalene-2-yl)anthracene (MNAn) have been reported as host materials, the new host having ortho-methylated naphthalene on the 2-position of the anthracene has increased charge transport ability due to increased π-electron density as well as a highly twisted structure, leading to excellent host behavior for blue OLEDs. We have designed a new asymmetrical anthracene derivative, *N*-(4-(10-naphthalene-2-yl)anthracene-9-yl)phenyl-*N*-phenylnaphthalene-2-amine, as a dopant. Generally, arylamine groups increase the hole transporting ability of the materials as well as reduce their crystallinity, improving device stability due to the amorphous structure, increase efficiency due to charge balance and reduce energy consumption due to reduced driving voltages [18]. Thus, anthracene derivatives containing arylamine have been reported, however, the reported compounds usually have a symmetrical structure because of their ease of synthesis. These symmetrically introduced arylamine groups usually deteriorate color purity for blue emission [13]. Therefore, we designed an asymmetrical anthracene derivative with an arylamine on the 9-position and naphthalene on the 10-position of the anthracene unit, respectively. These well matched host-guest materials can improve efficiency due to balanced energy levels and morphological stability due to similar structure based on twisted anthracene.

2. Experimental

2.1. Materials

All starting materials were purchased from Aldrich and Strem. All reagents purchased commercially were used without further purification.

2.2. Instrument

^{1}H NMR spectra were recorded using a Bruker Avance-300 MHz FT-NMR spectrometer, and chemical shifts were reported in ppm with tetramethylsilane as internal standard. FT-IR spectra were recorded using a Bruker IFS66 spectrometer. Thermogravimetric analysis (TGA) was performed under nitrogen using a TA instruments 2050 thermogravimetric analyzer. Differential scanning calorimeter (DSC) was conducted under nitrogen using a TA instrument DSC Q10. The both samples were heated using a 10 °C/min. UV-visible spectra and photoluminescence (PL) spectra were measured by Shimadsu UV-1065PC UV-visible spectrophotometer and Perkin Elmer LS50B fluorescence spectrophotometer, respectively. The electrochemical properties of the materials were measured by cyclic voltammetry (Epsilon C3) in a 0.1 M solution of tetrabutyl ammonium perchlorate in acetonitrile. The organic EL devices were fabricated using successive vacuum-deposition of *N*,*N*′-diphenyl-*N*,*N*′-bis-[4-(phenyl-m-tolylamino)-phenyl]-biphenyl-4,4′-diamine (DNTPD, 700 Å), *N*,*N*′-diphenyl-*N*,*N*′-di(1-napthyl)-1,1′-biphenyl-4,4′-diamine (NPD, 300 Å), 9.10-di(naphthalene-2-yl)anthracene (ADN): *p*-NAPPN (3%): or MNAn: *p*-NAPPN (3%), tris(8-hydroxyquinoline)aluminum (Alq3, 400 Å), LiF (5 Å), and Al electrode on top of the ITO glass substrate. The ITO glass with a sheet resistance of about 10 Ω was etched for the anode electrode pattern and cleaned in ultrasonic baths of isopropyl alcohol and acetone. The overlap area of Al and ITO electrodes is about 4 mm^2. A UV zone cleaner (Jeilight Company) was used for further cleaning before vacuum deposition of the organic materials. Vacuum deposition of the organic materials was carried out under a pressure of 2×10^{-7} torr. The deposition rate for organic materials was about 0.1 nm/s. The evaporation rate and the thickness of the film were measured with a quartz oscillator. OLED performance was studied by measuring the current–voltage–luminescence (*I*–*V*–*L*) characteristics, EL, and PL spectra at room temperature. *I*–*V*–*L* characteristics and CIE color coordinates were measured with a Keithley SMU238 and Spectrascan PR650. EL spectra of the devices were measured utilizing a diode array rapid analyzer system (Professional Scientific Instrument Corp.) Fluorescence spectra of the solutions in chloroform were measured using a spectro fluorimeter (Shimadzu Corp.).

2.3. Synthesis of naphthalene-2-yl boronic acid (**1**)

2.5 M *n*-butyllithium (80 mL, 31.9 mmol) was slowly added to 2-bromonaphthalene (60 g, 29.0 mmol) in tetrahydrofuran (THF) (100 mL) at −78 °C. The mixture was stirred for 30 min at −40 °C. Triethyl borate (127 g, 869.0 mmol) was slowly dropped into the mixture and stirred at room temperature. After 12 h, the reaction was terminated by the addition of 2 M HCl (200 mL) and extracted with dichloromethane (300 mL). The crude product was purified by recrystallization with hexane. Yield: 40 g (80%); mp. 268 °C, ^{1}H NMR (300 MHz, $CDCl_3$, ppm): 8.37(s, 1H), 8.18(s, 2H), 7.95–7.83 (m, 4H), 7.55–7.48 (m, 2H).

2.4. Synthesis of 9-(naphthalene-2-yl)anthracene (**2**)

9-Bromoanthracene (15 g, 58 mmol) and naphthalene-2-yl boronic acid (13 g, 76 mmol) was added in the mixture of toluene (80 mL), K_2CO_3 (40 mL), THF (25 mL) and of tetrakis(-triphenylphosphine) palladium (0) (0.27 g, 2 mol%). The solution was stirred in N_2 for 24 h at 110 °C. After reaction, the mixture was quenched with 2 N–HCl (400 mL). The crude product was extracted and dried. The purification was carried out by column chromatography with hexane. The product was purified by column chromatography with hexane as eluent Yield: 11.8 g (67%); m.p. 154 °C, ^{1}H NMR (300 MHz, $CDCl_3$, ppm): $\delta = 8.56$ (s, 1H). 8.02–8.11 (m, 4H), 7.91–7.96 (d, 2H), 7.70–7.73 (d, 2H), 7.57∼7.62 (m, 3H), 7.46–7.51 (m, 2H), 7.32–7.37 (m, 2H).

2.5. Synthesis of 9-bromo-10-(naphthalene-2-yl)anthracene (**3**)

In the 500 mL flask, of 9-(naphthalene-2-yl)-anthracene (20 g, 66 mmol), *N*,*N*-dimethylformamide (DMF) (30 mL) was stirred. *N*-bromosuccinimide (20 g, 0.12 mmol) was slowly dropped. After stirring for 7 h, water (700 mL) was added to the mixture. The crude product was filtrated and washed with ethanol. Yield: 16.9 g (67%); m.p. 173 °C, ^{1}H NMR (300 MHz, $CDCl_3$, ppm): 8.64–8.67 (d, 2H), 8.02–8.08 (m, 2H), 7.92 (d, 2H), 7.52–7.69 (m, 7H), 7.34 (m, 2H).

2.6. Synthesis of 4,4,4,5-tetramethyl-2-(10-(naphthalene-2-yl) anthracene-9-yl)-1,3,2-dioxaborolane (**4**)

2.5 M *n*-butyllithium (50.9 mmol) was slowly added to 9-bromo-10-(naphthalene-2-yl)anthracene (39.1 mmol) in THF (100 mL) at −78 °C. The mixture was stirred for 30 min at −40 °C. 2-Isopropoxy-4,4,5,5,-tetramethyl-[1, 2, 3] dioxaborolane (24 mL, 11.7 mmol) was slowly dropped into the mixture and stirred at room temperature. After 12 h, the reaction was terminated by the addition of 2 M HCl and extracted with ethyl acetate. The crude product was purified by column chromatography with hexane:ethyl acetate (10:1). Yield: 10 g (60.1%); ^{1}H NMR (300 MHz, $CDCl_3$, ppm) $\delta = 8.4$ (d, 2H), 8.07–8.01 (m, 2H), 7.9 (d, 2H), 7.6 (d, 2H), 7.6–7.5 (m, 2H), 7.54–7.49 (m, 3H), 7.33–7.28 (m, 2H), 1.6 (s, 12H).

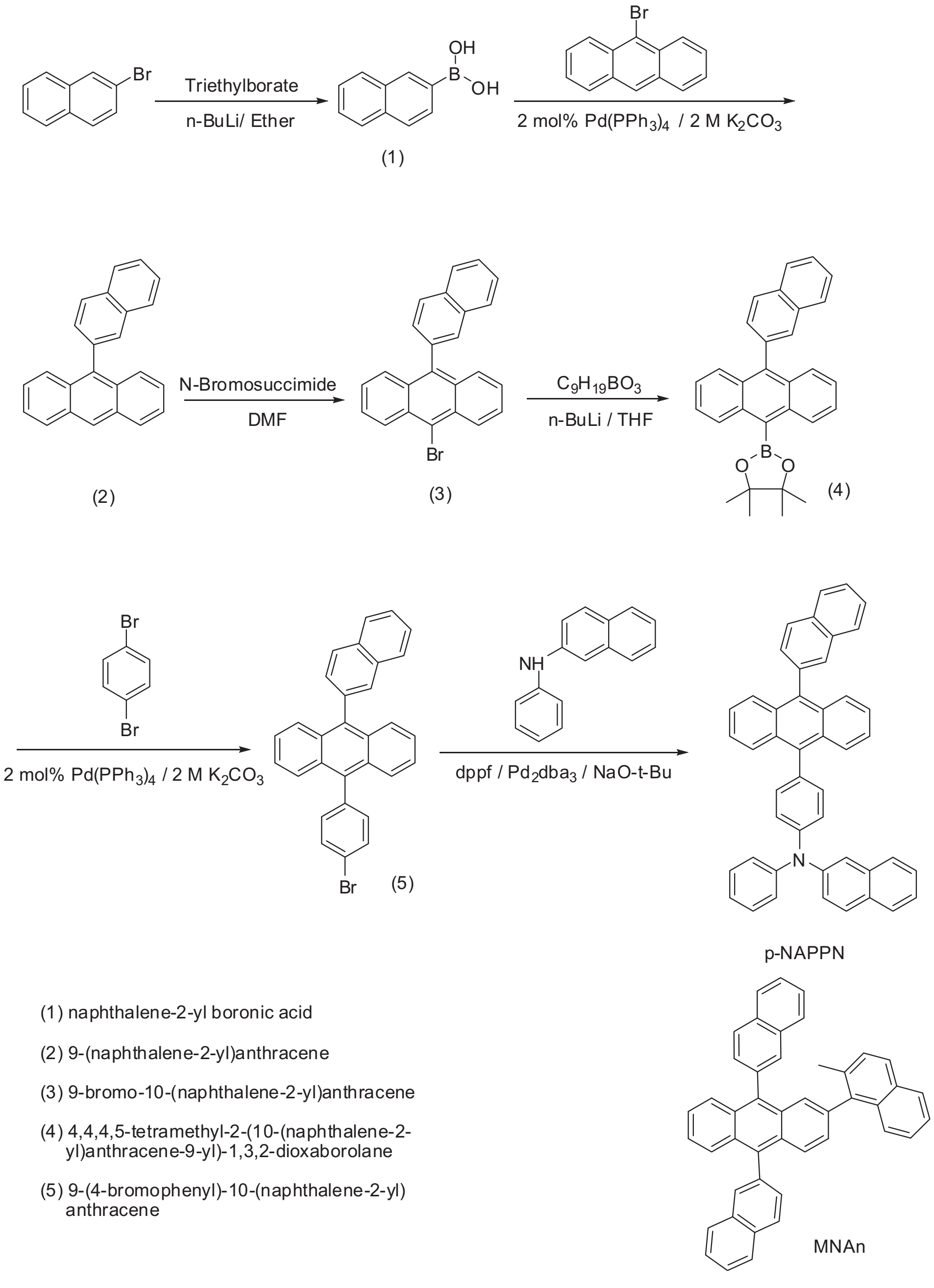

(1) naphthalene-2-yl boronic acid

(2) 9-(naphthalene-2-yl)anthracene

(3) 9-bromo-10-(naphthalene-2-yl)anthracene

(4) 4,4,4,5-tetramethyl-2-(10-(naphthalene-2-yl)anthracene-9-yl)-1,3,2-dioxaborolane

(5) 9-(4-bromophenyl)-10-(naphthalene-2-yl) anthracene

Scheme 1. Synthesis of *N*-(4-(10-naphthalene-2-yl)anthracene-9-yl)phenyl-*N*-phenylnaphthalene-2-amine (p-NAPPN).

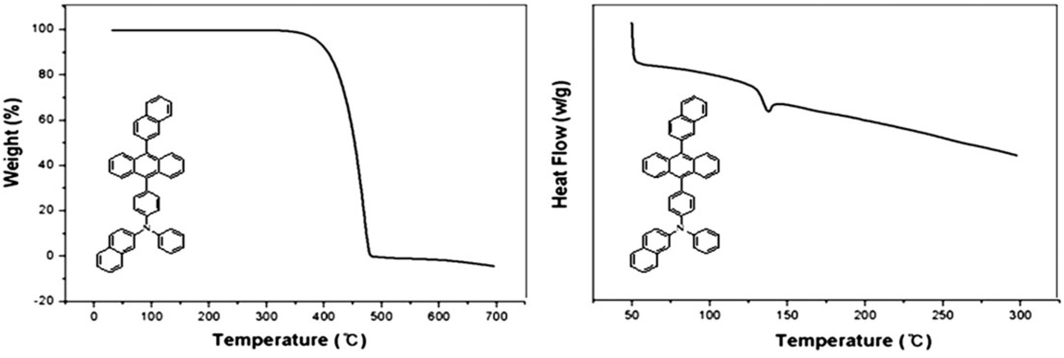

Fig. 1. TGA and DSC thermograms of p-NAPPN.

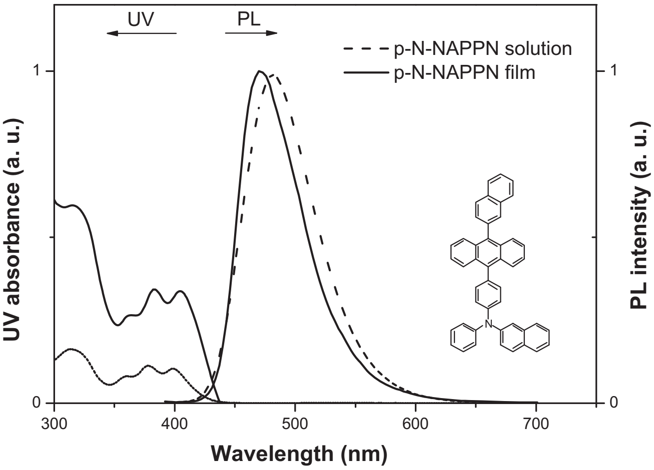

Fig. 2. UV–visible and PL spectra of p-NAPPN.

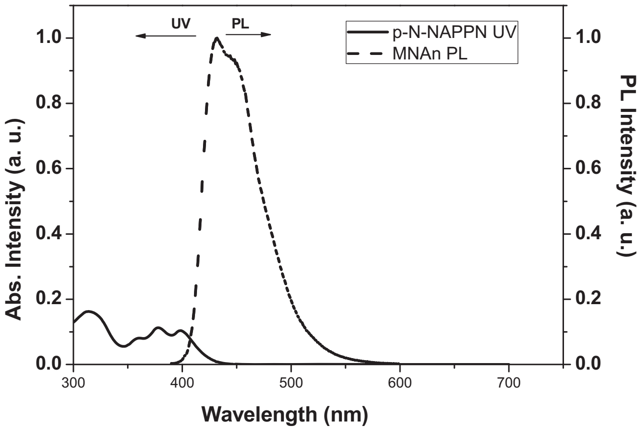

Fig. 3. PL spectrum of MNAn as an host and UV–vis absorption spectrum of p-NAPPN as a dopant.

*2.7. Synthesis of 9-(4-bromophenyl)-10-(naphthalene-2-yl) anthracene (**5**)*

1,4-Dibromobenzene (2 g, 8.5 mmol) and of 4,4,5,5-tetramethyl-2-(10-(naphthalene-2-yl)anthracene-9-yl)-1,3,2-dioxaborolane (2.56 g, 5.9 mmol) were added to solution of toluene (60 mL), 2 M K_2CO_3 (30 mL), 1 mol % of tetrakis(triphenylphosphine) palladium (0). The solution was stirring for 24 h at 90 °C. After reaction, the mixture was quenched with HCl (2 N, 400 mL). The crude product was extracted and dried. The purification was carried out by column chromatography with hexane and ethyl acetate (10:1) as eluent. Yield: 1.4 g (51%); m.p. 237 °C, ^{1}H NMR (300 MHz, $CDCl_3$, ppm): $\delta = 8.1$ (m, 2H), 8.0 (m, 2H), 7.9 (m, 2H), 7.7–7.6 (m, 6H), 7.6–7.4 (m, 5H), 7.4–7.2 (m, 4H) EI-MS: *m*/*z* 458.

2.8. Synthesis of N-(4-(10-naphthalene-2-yl)anthracene-9-yl) phenyl-N-phenylnaphthalene-2-amine (p-NAPPN)

Tris(dibenzylidenacetone)dipalladium (0) (Pd_2dba_3) (0.04 g, 0.05 mmol), 1,1-bis(diphenylphosphino)ferrocene (dppf) (0.04 g, 0.07 mmol), sodium tert-butoxide (0.4 g, 5 mmol) were added to toluene (40 mL). 9-(4-Bromophenyl)-10-(naphthalene-2-yl) anthracene (1.4 g, 3.0 mmol) was added to the mixture. After stirring 15 min, naphthalene-2-yl-phenyl amine (2.3 g, 8.1 mmol) was added to the mixture. After the mixture was refluxed for 24 h, H_2O added to the mixture to stop the reaction. The crude product was purified by recrystallization with toluene and ethanol. Yield: 0.8 g (44%); m.p. 274 °C, ^{1}H NMR (300 MHz, $CDCl_3$, ppm): $\delta = 8.0$ (m, 2H), 7.93–7.82 (m, 3H), 7.77 (q, 1H), 7.65 (d, 2H), 7.54–7.45 (m,3H), 7.35–7.21 (m, 9H), 7.09 (m, 1H), HRMS: calcd. for $C_{46}H_{31}N$: 597.2457, found: 597.2453. Anal. Calcd for $C_{46}H_{31}N$: C, 92.43; H, 5.23; Found: C, 92.40; H, 5.24.

2.9. Synthesis of 2-(2-methylnaphtathalene-1-yl)-9,10-di(naphthalene-2-yl)anthracene (MNAn)

The synthesis was followed by literature method. The product was purified by column chromatography with hexane as eluent. Yield: 1.96 g (29.17%); ^{1}H NMR (300 MHz, $CDCl_3$, ppm) $\delta = 8.17$–8.12 (m, 2H), 8.09–8.05 (m, 1H), 8.02–7.88 (m, 6H), 7.84–7.73 (m, 5H), 7.71–7.70 (m, 1H), 7.67–7.62 (m, 3H), 7.57–7.47 (m, 3H), 7.38–7.31 (m, 4H), 7.30–7.26 (m, 2H), 2.25 (d, 3H), HRMS: calcd. for $C_{45}H_{30}$: 570.2347, found: 570.2353.

3. Results and discussion

Scheme 1 displays the synthetic route used to prepare an asymmetrically arylamine substituted anthracene derivative as a dopant and the highly twisted ortho-substituted anthracene as a new host. 9-(4-Bromophenyl)-10-(naphthalene-2-yl)anthracene was obtained by Suzuki coupling reaction of 9-bromoanthracene naphthalene-2-yl boronic acid following bromination. *N*-(4-(10-naphthalene-2-yl)anthracene-9-yl)phenyl-*N*-phenylnaphthalene-2-amine (p-NAPPN) was synthesized by *N*-arylation with naphthalene-2-yl-phenyl-amine and 9-(4-bromophenyl)-10-(naphthalene-2-yl)anthracene. 2-Bromo-9,10-dinaphthyl anthracene was obtained by nucleophilic addition of 2-bromonaphthalene and 2-bromoanthraquinone followed by an oxidation reaction. MNAn was synthesized by a Suzuki coupling reaction of 2-bromo-9,10-dinaphthylanthracene with 2-methyl-1-naphthalene boronic acid. All compounds were purified by the silica column chromatographic method or recrystallization. Further purification was readily accomplished by sublimation under vacuum (10^{-6} Torr). The target compounds were characterized by NMR and mass spectroscopy.

The thermal properties of p-NAPPN were determined by differential scanning calorimetry (DSC) and thermogravimetry (TGA) measurements. (Fig. 1) MNAn and p-NAPPN exhibit high thermal stabilities with decomposition temperatures (5% weight

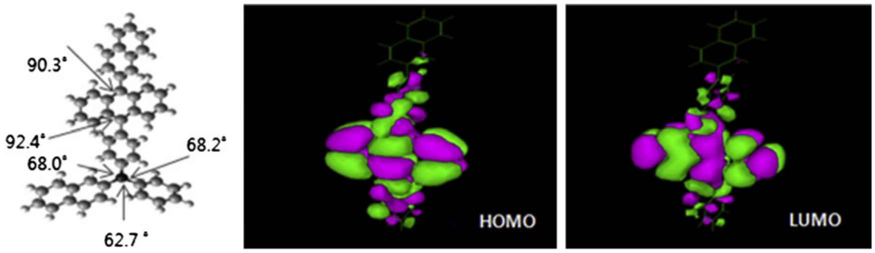

Fig. 4. Contour plots regarding the HOMO and LUMO of p-NAPPN.

Table 1
The optical, thermal and electrical properties of MNAn and p-NAPPN.

	Solution[a]		Film[a]		HOMO (eV)	LUMO (eV)	Eg[b] (eV)	T_d (°C)	T_m (°C)	T_g (°C)
	UV (nm)	PL (nm)	UV (nm)	PL (nm)						
MNAn	361,381,402	431	364,385,406	454	5.58	2.60	2.98	382	292	–
p-NAPPN	361,377,401	481	382	470	5.54	2.66	2.88	388	274	135

[a] In $CHCl_3$.
[b] The optical energy band gap.

loss) of 382 °C and 388 °C. The melting transition temperature (T_m) of MNAn was observed at 292 °C.[30] Tg and Tm of p-NAPPN are 135 and 274, respectively. The high thermal stability of these two compounds as well as similar structures inhibited self-aggregation. This suggests that the emitting layer composed with MNAn and p-NAPPN has stable morphological properties, which is desirable for OLEDs with high stability and efficiency.

Fig. 2 shows the UV–visible absorption and photoluminescence (PL) spectra of p-NAPPN in chloroform solution. The UV–visible absorption spectrum of p-NAPPN shows the characteristic vibrational patterns of an isolated anthracene group (λ_{max} = 361, 377, 401 nm). Upon irradiation at 365 nm, the PL spectrum of p-NAPPN in solution exhibited an excellent blue emission with the peak maximum at λ_{max} 481 nm. In the PL spectrum of p-NAPPN in a film, the peak maximum of the blue emission is found at 470 nm without a shoulder emission, which implies the blue emission with inhibited intermolecular interaction. p-NAPPN containing an aryl amine group showed a blue shifted emission in the thin film, which is often observed for arylamine derivatives [31]. Fig. 3 represents the PL spectrum of MNAn as a host and UV–vis absorption spectrum of p-NAPPN as a dopant. From this result, it can be suggested that the efficient energy transfer can occur by the close match of emission spectrum of the host and the absorption spectrum of guest.

The optical energy band gap of MNAn and p-NAPPN is 2.98 eV and 2.88 eV, respectively, calculated from the threshold of the optical absorption (416 nm for MNAn, 430 nm for p-NAPPN). From these results, it is speculated that efficient Foster energy transfer takes place, because the band gap of p-NAPPN is smaller than that of the MNAn host.

A contour plot regarding the HOMO and LUMO of p-NAPPN determined by theoretical calculation is shown in Fig. 4. While the electron density of the HOMO of p-NAPPN is slightly spread to the arylamine, the electron density of the LUMO is largely concentrated on anthracene unit.

Cyclic voltammetry (CV) was carried out to identify the electrochemical behavior of p-NAPPN. MNAn, containing methylnaphthalene, has a slightly higher oxidation potential (Eox) and a higher energy gap than those of p-NAPPN which contains an electron donating p- arylamine group. The HOMO levels of MNAn and p-NAPPN were 5.58 eV and 5.54 eV, respectively. The LUMO values of MNAn and p-NAPPN were 2.60 and 2.66 eV, respectively, which were calculated from the optical band gap and HOMO values. Table 1 summarized the optical, thermal and electrochemical results of MNAn and p-NAPPN.

To study the electroluminescence performance of MNAn and p-NAPPN, two different types of blue emitting device have been fabricated. Multilayer devices with a configuration of indium tin oxide (ITO)/*N*,*N*′-diphenyl-*N*,*N*′-bis-[4-(phenyl-*m*-tolylamino) phenyl]-biphenyl-4,4′-diamine (DNTPD, 70 nm)/1,4-bis[(1-naphthylphenyl)amino]biphenyl (α-NPD) (50 nm)/ADN:p-NAPPN (3%)/ tris(8-hydroxyquinoline) aluminum (Alq3, 40 nm)/LiF (0.5 nm)/ Al (device A) and (ITO)/DNTPD (70 nm)/1,4-bis[(1-naphthyl phenyl)-amino]biphenyl (α-NPD) (50 nm)/MNAn:p-NAPPN (3%)/ tris(8-hydroxyquinoline) aluminum (Alq3, 40 nm)/LiF (0.5 nm)/Al

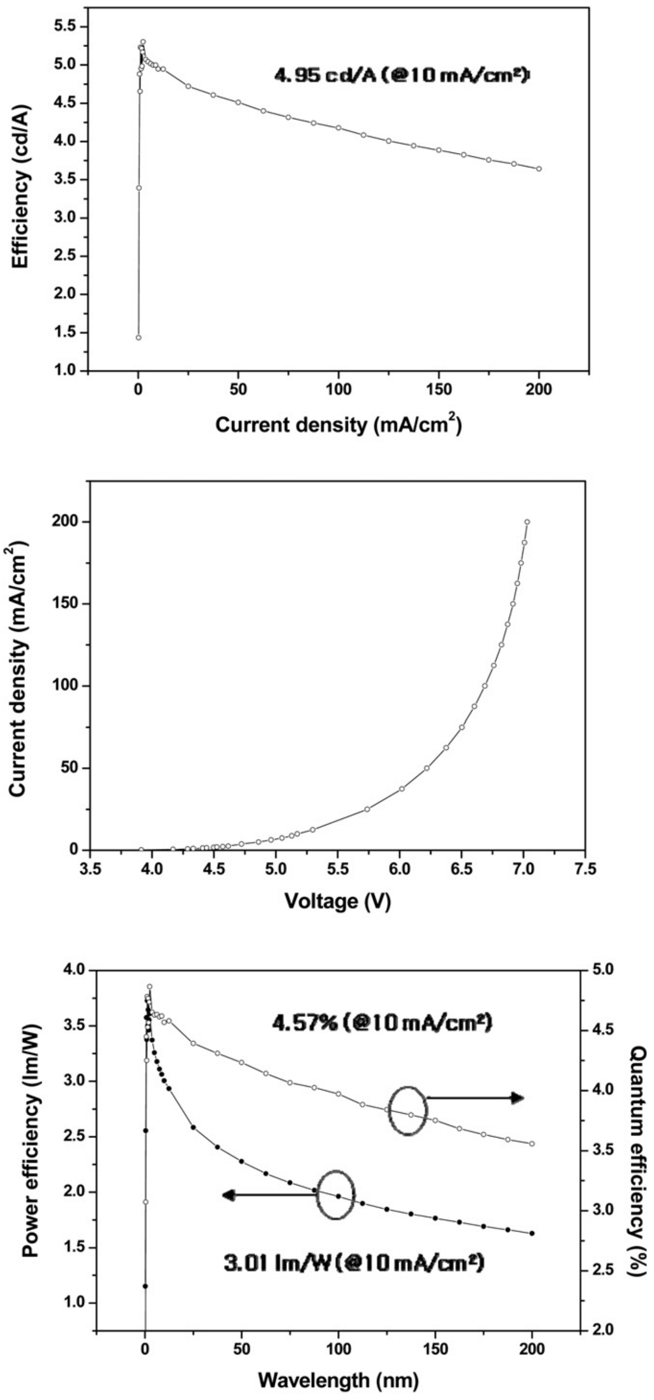

Fig. 5. The voltage versus current density characteristics, luminous efficiency (LE), power efficiency (PE), and external quantum efficiency (EQE) of device A.

Table 2
EL performances of devices Device A: (ITO)/DNTPD (70 nm)/(α-NPD) (50 nm)/ADN:p-NAPPN (3%)/(Alq3, 40 nm) /LiF (0.5 nm)/Al. Device B: (ITO)/DNTPD (70 nm)/(α-NPD) (50 nm)/MNAn:p-NAPPN (3%)/(Alq3, 40 nm) /LiF (0.5 nm)/Al.

Device	Dopant	Host	λ_{max} (nm)	η_c (cd A^{-1})[a]	η_P (lm W^{-1})[b]	η_{exp} (%)[c]	CIE (*x*, *y*)
Device A	p-NAPPN	ADN	456	4.95	3.01	4.57	0.15, 0.14
Device B		MNAn	464	6.88	4.37	5.31	0.14, 0.18

[a] Current efficiency (η_c).
[b] Power efficiency (η_P).
[c] External quantum efficiency (η_{exp}).

(device B) were fabricated, where ITO serves as the anode and Al as the cathode. The stack of organic layers consists of DNTPD as a hole injection layer, α-NPD as a hole-transport layer, ADN doped with p-NAPPN (3%) as the emitter or MNAn doped with p-NAPPN as the emitter, Alq3 as an electron-transport layer, and LiF as an electron-injection layer. In this study, ADN was used as the host for comparing MNAn in blue-emitting electroluminescence devices.

Fig. 5 shows the voltage versus current density characteristics, luminous efficiency (LE), power efficiency (PE), and external quantum efficiency (EQE) of device A. The EL properties of the devices are summarized in Table 2. The turn on voltage was around 4.1 V for device A. The current efficiency, power efficiency, and external quantum efficiency of device A at 10 mA was 4.95 cd/A, 3.01 lm/W and 4.57%, respectively. Fig. 6 shows EL spectrum of device A. The EL maximum and full width at half maximum (FWHM) of device A were 456 nm and 50 nm, respectively. The CIE coordinates of device A was (0.15, 0.14). From the results, the newly developed p-NAPPN has potential to be used as a highly efficient pure blue color dopant.

Fig. 7 shows the voltage versus current density characteristics, luminous efficiency (LE), power efficiency (PE), and external quantum efficiency (EQE) of device B. The current efficiency, power efficiency, and external quantum efficiency of device B at 10 mA was 6.88 cd/A, 4.37 lm/W and 5.31%, respectively. The maximum EQE of device B was greater than 5%, the known theoretical limit. The electroluminescence in the host-dopant system can occur by the Foster-type energy transfer from the host to dopant. As expected based on the band gap, Foster-type energy transfer can effectively occur when the band gap of the host is higher than that of the guest. It has been reported that the band gap of ADN is 3.1 eV. Although the ADN host has a higher band gap than that of MNAn, the EL efficiency of device B was 1.5 times higher than that of device A. It can be seen from Fig. 2 that the absorption spectrum of the p-NAPPN dopant material overlapped better with the emission spectra of MNAn than that of ADN, demonstrating that p-NAPPN can effectively accept energy transfer from the MNAn host material

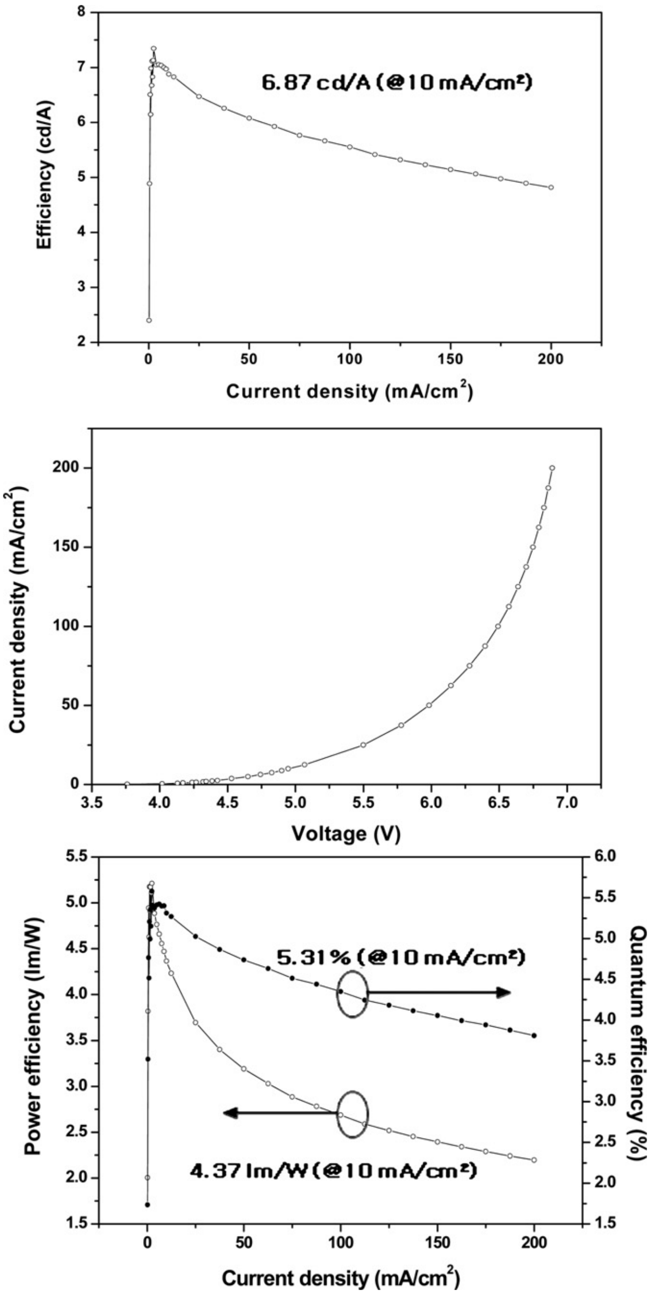

Fig. 7. The voltage versus current density characteristics, luminous efficiency (LE), power efficiency (PE), and external quantum efficiency (EQE) of device B.

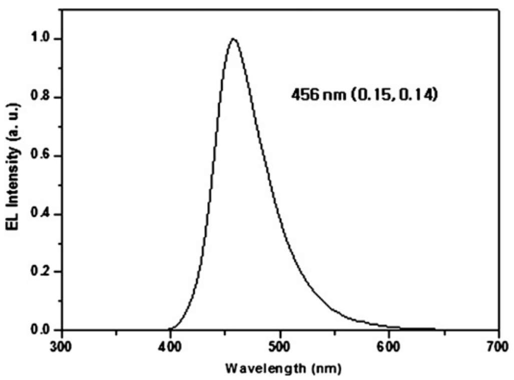

Fig. 6. EL spectrum of device A.

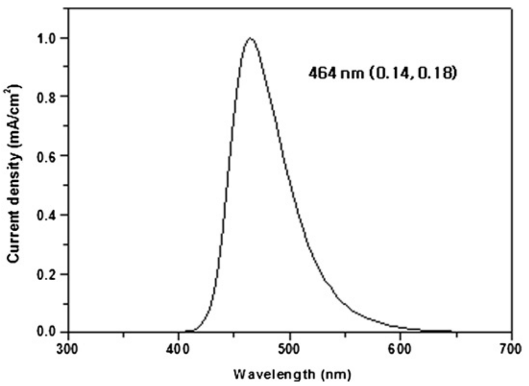

Fig. 8. EL spectrum of device B.

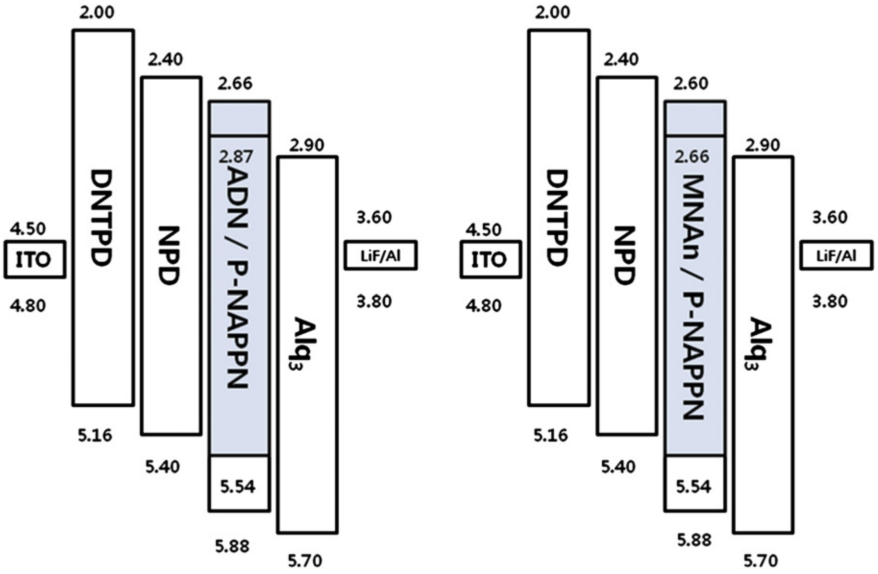

Fig. 9. Energy level diagrams of devices.

by a Foster-type energy transfer, thereby leading to improved EL efficiencies. Furthermore, it is suggested that the energy levels are well matched in device B. The proposed energy level diagrams of the devices are shown in Fig. 8. Device A used ADN as a host and p-NAPPN as a dopant and had a higher hole injection barrier (0.48 eV) from the HOMO of NPD to that of the ADN host than the electron injection barrier from the LUMO of Alq3 to that of the ADN host (0.03 eV). Thus, it is suggested that the electrons are injected into the LUMO of the ADN host, meanwhile, holes are injected to p-NAPPN because the energy barrier between the HOMO level of p-NAPPN and the HOMO level of NPD is only 0.14 eV and the doping ratio is 3%. Thus, it is suggested that charge trapping emission takes place. On the other hand, Device B used MNAn as a host and p-NAPPN as a dopant, and the HOMO and LUMO levels of the dopant p-NAPPN are included with those of the host MNAn. Foster energy transfer can thus effectively occur in device B owing to the well matched energy levels. Fig. 9 shows the EL spectrum of device B. The EL maximum of device B and FWHM was 464 nm and 56 nm, respectively. The CIE coordinates of device B were $x = 0.14$, $y = 0.18$.

4. Conclusion

We have designed an asymmetrically highly twisted ortho-substituted anthracene derivative as a wide energy gap host and an asymmetrically arylamine substituted anthracene derivative as a dopant for blue emitting OLEDs. The new host and dopant have good thermal stability with a high Tg despite being small molecules. A multilayer organic EL device constructed using the developed p-NAPPN-doped ADN as the emitting layer produced a bright blue emission with a narrow FWHM of 50 nm. The device achieved maximum quantum efficiency of 4.57% (power efficiency of 3.01 lm/W, current efficiency of 4.95 cd/A and exhibits a blue CIE (Commission Internationale de l'Eclairage) chromaticity coordinates $x = 0.15$, $y = 0.14$. The fabricated device structured with (ITO)/DNTPD (70 nm)/(α-NPD) (50 nm)/MNAn:p-NAPPN (3%)/(Alq3, 40 nm)/LiF (0.5 nm)/Al using MNAN as a host and p-NAPPN as a dopant showed 6.88 cd/A current efficiency, 4.37 lm/W power efficiency, and 5.31% of external quantum efficiency at 10 mA. The high efficiency of the device with the new host and dopant may be attributed to not only the significant overlap between the absorption spectrum of p-NAPPN and the photoluminescence spectrum of MNAn but also the well matched energy levels of the dopant and host, allowing efficient host-to-guest Foster energy transfer and consequently greatly improved luminance efficiency.

Acknowledgement

This research was financially supported by Basic Science Research Program through the National Research Foundation of Korea (NRF) funded by the Ministry of Education, Science and Technology (2011-0003336).

Il Kang, Seul-ong Kim and Hyuntae Park thank to MKE and KIAT through the Workforce Development Program in Strategic Technology Under Ministry of Knowledge Economy of Korea.

References

[1] Wu MF, Yeh SJ, Chen CT, Murayama H, Tsuboi T, Li WS. The quest of high-performance host materials for electrophosphorescence blue dopants. Adv Funct Mater 2007;17:1887–95.
[2] Tang CW, Vanslyke SA. Organic electroluminescence diode. Appl Phys Lett 1987;51:913–5.
[3] Kang DM, Kang JW, Kim YH, Shin SC, Kim JJ, Kwon SK. Iridium complexes with cyclometalated 2-cycloalkenyl-pyridine ligands as highly efficient emitters for organic light-emitting diodes. Adv Mater 2008;20:2003–7.
[4] Park YS, Kang JW, Kang DM, Kim YH, Kwon SK, Kim JJ. Efficient, color stable white organic light-emitting diode based on high energy level yellowish-green dopants. Adv Mater 2008;20:1957–61.
[5] Shih HT, Lin CH, Shih HH, Cheng CH. High-performance blue electroluminescent devices based on a biaryl. Adv Mater 2002;14:1409–12.
[6] Jang JW, Park H, Shin MK, Jung SO, Kwon SK, Kim YH. Novel quinoxaline derivatives containing arylaminated aceanthrylene for organicred-light emitting diodes. Dyes and Pigments 2011;88:44–9.
[7] Kim SO, Zhao Q, Thagaraju K, Kim JJ, Kim YH, Kwon SK. Synthesis and characterization of solution-processable highly branched Iridium(III) complex cored dendrimer based on tetraphenylsilane dendron for host-free green phosphorescent organic light emitting diodes. Dyes and Pigments 2011;90: 139–45.
[8] Chiechi RC, Tseng RJ, Marchioni F, Yang Y, Wudl F. Efficient blue-light-emitting electroluminescent devices with a robust fluorophore: 7,8,10-triphenylfluoranthene. Adv Mater 2006;18:325–8.
[9] Shih PI, Tseng YH, Wu FI, Dixit AK, Shu CF. Stable and efficient white electroluminescent devices based on a single emitting layer of polymer blends. Adv Funct Mater 2006;16:1582–9.
[10] Li ZH, Wong MS, Fukutani H, Tao Y. Full emission color tuning in bis-dipolar diphenylamino-endcapped oligoarylfluorenes. Chem Mater 2005;17: 5032–40.

[11] Zhao Z, Lu JH, Yang Y. Fluorescent. Carrier-trapping dopants for highly efficient single-layer polyfluorene LEDs. Adv Funct Mater 2007;17:2203–10.

[12] Zhang CJ, Zhao WM, Wang ZQ, Huang D, Ye Y, Ou XM, et al. Highly efficient non-doped deep-blue organic light-emitting diodes based on anthracene derivatives. J Mater Chem 2010;20:1560–6.

[13] Pu YJ, Kamiya A, Nakayama K, Kido J. Arylamino-9,10-diphenylanthracenes for organic light emitting devices. Org Electron 2010;11:479–85.

[14] Lee KH, Kang LK, Lee JY, Kang S, Jeon SO, Yook KS, et al. Molecular engineering of blue fluorescent molecules based on silicon end-capped diphenylamino-fluorene derivatives for efficient organic light-emitting materials. Adv Funct Mater 2010;20:1345–58.

[15] Gao ZQ, Li ZH, Xia PF, Wong MS, Cheah KW, Chen CH. Efficient deep-blue organic light-emitting diodes: arylamine-substituted oligofluorenes. Adv Funct Mater 2007;17:3194–9.

[16] He F, Tian L, Xie W, Li M, Gao Q, Hanif M, et al. Highly efficient blue organic light-emitting devices based on improved Guest/Host Combination. J Phys Chem C 2008;112:12024–9.

[17] Baldo MA, O'Brien DF, Thompson ME, Forrest SR. Excitonic singlet-triplet ratio in a semiconducting organic thin film. Phys Rev B; 1999:14422–8.

[18] Kim YH, Shin DC, Kim SH, Ko CH, Yu HS, Chae YS, et al. Novel blue emitting material with high color purity. Adv Mater 2001;13:1690–3.

[19] Kim YH, Jung HC, Kim SH, Yang KY, Kwon SK. High-purity-blue and high efficiency electroluminescence devices based on anthracene. Adv Funct Mater 2005;15:1799–805.

[20] Park JW, Kim YH, Jung SH, Byeon KN, Shin SC, Kwon SK. Efficient and stable blue organic light-emitting diode based on an anthracene derivative. Thin Solid Films 2008;516:8381–5.

[21] Kim YH, Lee SJ, Byeon KN, Kim JS, Shin SC, Kwon SK. Efficient blue light emitting diode by using anthracene derivative with 3,5-diphenylphenyl wings at 9- and 10-position. Bull Korean Chem Soc 2007;28:443–4.

[22] Park JW, Kang P, Park H, Oh HY, Yang JH, Kim YH, et al. Synthesis and properties of blue-light-emitting anthracene derivative with diphenylamino-fluorene. Dyes Pigments 2010;85:93–8.

[23] Shih PI, Chuang CY, Chien CH, Diau EW, Shu CF. Highly efficient non-doped blue-light-emitting diodes based on a anthracene derivative end-capped with tetraphenylethylene groups. Adv Funct Mater 2007;17:3141–6.

[24] Kim SK, Yang B, Ma Y, Lee JH, Park JW. Exceedingly efficient deep-blue electroluminescence from new anthracenes obtained using rational molecular design. J Mater Chem 2008;18:3376–84.

[25] Park JK, Lee KH, Kang S, Lee JY, Park JS, Seo JH, et al. Highly efficient blue-emitting materials based on 10-naphthylanthracene derivatives for OLEDs. Org Electron 2010;11:905–15.

[26] Wang Jr S, Oldham Jr WJ, Hugack RA, Bazan GC. Synthesis, morphology, and optical properties of tetrahedral oligo(phenylenevinylene) materials. J Am Chem Soc 2000;122:5695–709.

[27] Wu KC, Ku PJ, Lin CS, Shin HT, Wu FK, Huang MJ, et al. The photophysical properties of dipyrenylbenzenes and their application as exceedingly efficient blue emitters for electroluminescent devices. Adv Funct Mater 2007;18:67–75.

[28] Kim JU, Lee HB, Shin JS, Kim YH, Joe YK, Oh HY, et al. Synthesis and characterization of new blue light emitting material with tetraphenylsilyl. Syn Met 2005;150:27–32.

[29] Daniel K, Huang TH, Lin JT, Tao YT, Chuen CH. Blue-emitting anthracenes with end-capping diarylamines. Chem Mater 2002;14:3860–5.

[30] Shin MK, Kim SO, Park HT, Park SJ, Yu HS, Kim YH, et al. Synthesis and characterization of ortho-twisted asymmetric anthracene derivatives for blue organic light emitting diodes. Dyes and Pigments, doi:10.1016/j.dyepig.2011.03.002.

[31] Li HC, Hu YF, Zhang YG, Ma DG, Wang LX, Jing XB, et al. Novel thermally stable blue-light-emitting polymer containing *N*, *N*, *N*′ *N*′-tetraphenyl-phenylenediamine units and its intramolecular energy transfer. Chem Mater 2002;14:4484–6.